

A Rectangular Tetrahedral Adaptive Mesh Based Corotated Finite Element Model for Interactive Soft Tissue Simulation

Kazuyoshi Tagawa¹, Takahiro Yamada¹, and Hiromi T. Tanaka¹

Abstract— In this paper, we propose a rectangular tetrahedral adaptive mesh based corotated finite element model for interactive soft tissue simulation. Our approach consists of several computation reduction techniques. They are as follows: 1) an efficient calculation approach for computing internal forces of nodes of elastic objects to take advantage of the rectangularity of the tetrahedral adaptive mesh; 2) fast shape matching approach by using a new scaling of polar decomposition; 3) an approach for the reduction of the number of times of shape matching by using the hierarchical structure.

We implemented the approach into our surgery simulator and compared the accuracy of the deformation and the computation time among 1) proposed approach, 2) L-FE, and 3) NL-FEM. Finally, we show the effectiveness of our proposed approach.

I. INTRODUCTION

Computationally efficient deformation simulations of organs are required for surgery training systems. This necessity is increased especially in the case of presenting reaction forces (e.g. reaction forces while touching or grasping the organs). This is because a higher update rate (about several hundred [Hz]) of deformation simulation is required for stable force presentation.

To date, as typical deformation models for elastic objects; 1) the mass spring model (MSM) [1] and 2) the finite element method (FEM) [2] have been proposed. The MSM is often solved by different methods (e.g. Euler method) and computation time of the MSM per step is low. However, a higher update rate of the simulation is required. Furthermore, the relationship between spring constants and physical properties of real elastic objects is not clear. In contrast with MSM; FEM is based on continuum mechanics. Simulation results using FEM works well with real elastic objects. However, computation cost of FEM is high because FEM is often solved by large scale simultaneous equations and implicit methods (e.g. backward Euler method). Thus, in any case, computation cost of deformation simulations of the organs becomes a problem.

In addition, because large deformations which involve rotations often occur in organs during surgery [3-4], deformation simulations for the surgery simulator must satisfy the ability to consider geometric nonlinearity. Thus, computationally efficient deformation simulations which are based on continuum mechanics and can consider geometric nonlinearity are required.

One such deformation model, Saint Venant Kirchhoff (StVK) Model was proposed. Delingette [5] and Kikuuwe et al. [6] proposed computationally efficient simulation approaches for the StVK Model. They modeled the StVK Model by biquadratic and quadratic springs, and used it to compute object deformation. However, acceleration as the theoretical value is not realized due to a delay caused by random memory access in the computation.

Recently, in the field of computer graphics, corotated FEM [7] has been proposed. In corotated FEM shape matching between tetrahedral elements before deformation and the tetrahedral elements after deformation is performed to define the local coordinate system of each tetrahedral element and remove component of rotational motion. The deformation calculation using a linear deformation model is performed on the local coordinate system thus geometric nonlinearity has become possible. However, there is a problem that a large amount of computation is required for this matching (extraction of the component of the rotational motion) [8].

Also, as other acceleration approaches, 1) multi-resolution models [9-11] and 2) parallel computation approaches [12-16] have been proposed. By applying these approaches to the above models, further acceleration can be expected.

In this paper, a novel efficient computation approach for corotated FEM is proposed. We introduce and state several computation reduction techniques. These are as follows. 1) An efficient calculation approach for computing internal forces of nodes of elastic objects to take advantage of the rectangularity of the tetrahedral adaptive mesh [17] in a binary tree based multi-resolution model. 2) Fast shape matching (extraction of the component of the rotational motion) approach using a polar decomposition method proposed by Byers [18]. 3) An approach to reduce of the number of times of shape matching. This is realized by substituting the rotation of tetrahedra at deep depth for rotation of tetrahedra at shallow depth.

In our evaluation experiment, we compare the accuracy of deformation and computation time among 1) proposed approach, 2) linear finite element model (L-FEM), and 3) nonlinear finite element model (NL-FEM). Then, we show the effectiveness of our proposed approach.

II. MULTI-RESOLUTION DEFORMATION MODEL

We proposed a multi-resolution model using a tetrahedral adaptive mesh [17].

In the tetrahedral adaptive mesh generation the 3D region (elastic object) is initially enclosed with six root tetrahedra as shown in Figure 1. Then, according to local field properties (e.g. material properties or curvatures of isosurfaces) observed at the nodes the root tetrahedra are recursively bisected (subdivided at the middle point of the longest edge of the

¹K. Tagawa, T. Yamada, and H. T. Tanaka are with Ritsumeikan University, 1-1-1 Noji-higashi, Kusatsu-shi, Shiga, Japan (corresponding author to provide phone: +81-77-599-4307; fax: +81-50-5552-3211; e-mail: tagawa@tagawa.info).

tetrahedra) independently in the region of rapid field variation. This subdivision process is repeated until the entire volume is approximated with the given accuracy criterion. At the same time object surfaces are constructed using the marching tetrahedra method [19].

In online re-mesh deformation simulation each tetrahedron is recursively refined (bisected) or simplified according to the rate of elongation σ of the longest edge of the tetrahedron.

The advantages of our online re-mesh approach using the tetrahedral adaptive mesh are as follows. 1) Low computation cost: Computational complexity of these processes is $O(\log n)$, because neighboring regions considered in the subdivision is limited. 2) High quality mesh: In our approach only three types of tetrahedra are used (Figure 2). The lower limit of aspect ratio of these tetrahedra is 0.64. The upper limit of the radius-shortest edge ratio of these tetrahedra is 1.11.

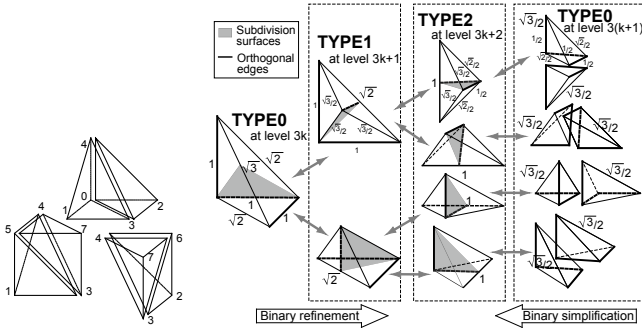


Figure 1. Six root tetrahedral.

Figure 2. Binary refinement and simplification.

III. RECTANGULAR TETRAHEDRAL ADAPTIVE MESH BASED COROTATED FEM

In this section, at first, we explain an overview of corotated FEM. Then, we propose 1) an efficient calculation approach for computing internal forces of nodes of elastic objects taking advantage of rectangularity of the tetrahedral adaptive mesh [17] in a binary tree based multi-resolution model. 2) Fast shape matching (extraction of the component of rotational motion) approach using a polar decomposition method proposed by Byers [18]. 3) An approach to reduce shape matching which is realized by substituting the rotation of tetrahedra at deep depth for rotation of tetrahedra at shallow depth.

A. Overview of Corotated Finite Element Model

In linear FEM, the relationship between elastic force vector f_T^L of nodes of tetrahedron T and displacement vector u_T of nodes of tetrahedron T is described by a linear equation, as follows:

$$K_T u_T = f_T^L \quad (1)$$

where K_T is a stiffness matrix of tetrahedron T.

In contrast, in the corotated FEM, elastic force f_T^C is calculated by

$$R_T K_T (R_T^{-1} x_T - x_{0,T}) = f_T^C, \quad (2)$$

where R_T , x_T and $x_{0,T}$ are a rotation matrix of tetrahedron T, a position vector of nodes of tetrahedron T and an initial position vector of nodes of tetrahedron T respectively. At this time the computational cost of extraction of R_T and the calculation of the whole equation (2) becomes a problem. Figure 3 shows the calculation process of the corotated FEM.

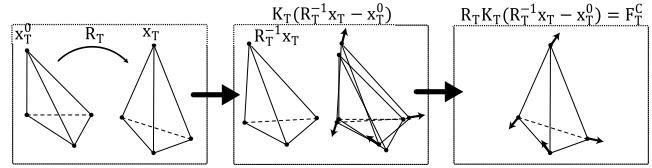


Figure 3. Calculation process of corotated FEM.

B. Efficient Calculation Approach for Internal Forces-Taking Advantage of Rectangularity of Tetrahedra

In equation (2), the elastic force is calculated using the stiffness matrix K_T of tetrahedron T. As shown in Figure 2, our tetrahedral adaptive mesh only consists of three types of shapes of rectangular tetrahedra. Therefore, we propose an efficient calculation approach to take advantage of this orthogonality.

We define local coordinate systems which along with orthogonal axes of these rectangular tetrahedra are shown in Figure 2. Using these local coordinate systems, 49 [%] of elements of the stiffness matrix K_T of tetrahedron (TYPE0) become 0, 28 [%] of elements of the stiffness matrix K_T of tetrahedron (TYPE1) become 0, and 39 [%] of elements of the stiffness matrix K_T of tetrahedron (TYPE2) become 0. Thus, acceleration approximately proportional to these ratios is possible.

C. Fast Shape Matching Approach Using Byers' Polar Decomposition

In corotated FEM, extraction of the rotation matrix R_T is required. A translation matrix A which contains rotation and stretching parts of tetrahedron T is expressed as follows:

$$\begin{bmatrix} A & t \\ 0 & 0 & 0 & 1 \end{bmatrix} = \begin{bmatrix} q_{1x} & q_{2x} & q_{3x} & q_{4x} \\ q_{1y} & q_{2y} & q_{3y} & q_{4y} \\ q_{1z} & q_{2z} & q_{3z} & q_{4z} \\ 1 & 1 & 1 & 1 \end{bmatrix} \begin{bmatrix} p_{1x} & p_{2x} & p_{3x} & p_{4x} \\ p_{1y} & p_{2y} & p_{3y} & p_{4y} \\ p_{1z} & p_{2z} & p_{3z} & p_{4z} \\ 1 & 1 & 1 & 1 \end{bmatrix}^{-1}, \quad (3)$$

where p and q are position vectors of nodes in the undeformed tetrahedron T and position vector of nodes in the deformed tetrahedron T respectively.

In this paper, we used Byers' polar decomposition approach [18] for the extraction of the rotation part. The following iterative computation (equation 4) is performed until a convergence condition $r < \sigma$ is satisfied, where σ is threshold of the convergence. The variables a and b in equation 5 are determined by $a \leq \|X_0^{-1}\|_2^{-1}$ and $b \geq \|X_0\|_2$, respectively.

$$X_{k+1} = \frac{1}{2} (\zeta_k X_k + \zeta_k^{-1} X_k^{-*}) \quad (4)$$

$$\zeta_0 = \frac{1}{\sqrt{ab}}, \zeta_1 = \sqrt{\frac{2}{\sqrt{\frac{b}{a}} + \sqrt{\frac{a}{b}}}}, \zeta_k = \sqrt{\frac{2}{\zeta_{k-1} + \zeta_{k-1}^{-1}}} \quad (5)$$

$$r = \|X_k - X_k^*\|_F \quad (6)$$

D. Shape Matching Computation Reduction Using Hierarchical Structure

As stated in the subsection above, the computational cost of shape matching is still high when using efficient polar decomposition. Therefore, we propose an approach to reduce the amount of computation of shape matching using the hierarchical structure of the binary tree of the tetrahedral adaptive mesh.

In tetrahedral adaptive mesh generation, as shown in Figure 1 and Figure 2, the six root tetrahedra are recursively bisected and then the binary tree is constructed. In this process, two child tetrahedra are generated from one parent tetrahedron and four grandchild tetrahedra are generated from one parent tetrahedron and so on. Therefore rotation matrices of these child or grandchild or descendant tetrahedra are similar to their ancestor tetrahedra.

We propose an approach for the reduction of the number of times of shape matching. This is realized by substituting the rotation matrices of descendant tetrahedra for rotation matrices of ancestor tetrahedra.

IV. EVALUATION EXPERIMENT

A. Evaluation Model

Figure 4 shows an initial tetrahedral mesh (all tetrahedra were TYPE0, subdivision levels of the tetrahedra were 6) of a soft tissue model which was used in this evaluation experiment, and Table 1 shows detailed information of the model. As shown in Figure 4, the model was rectangular shaped and its size was $64 \times 64 \times 192$ mm. A fixed boundary condition was applied to nodes on a plane ($z=0$). We set Young's modulus $E=0.5$ kPa, Poisson's ratio $\nu=0.49$, and density $\rho=10$ Kg/m³. We used $\sigma=3.85e-5$ as the threshold of r in equation (6). We applied acceleration of gravity $g=9.8$ m/s² (negative direction of y axis) to all nodes of the model.

In this experiment, we used a PC (CPU: Intel Xeon w3530 2.8 GHz, Memory:8 GB, OS:Scientific Linux release 6.1).

We compared the accuracy (error) of deformation and computation time among 1) proposed approach, 2) linear FEM (L-FEM), and 3) nonlinear FEM (NL-FEM).

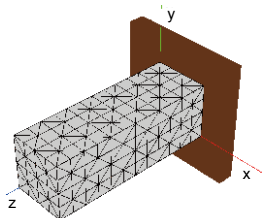


Figure 4. Experimental Model.

Table1. Detail of Experimental Model.

number of nodes	325
number of tetrahedra	1152

B. Evaluation Result

Figure 5 shows computation time of each model. The "Level 3's R" shows the results of corotated FEM whose rotation matrices were substituted by the rotation matrices of their ancestor tetrahedra (in case of "Level 3's R", its subdivision level was 3). As shown in Figure 5, we can see that the computation times of calculated rotations are drastically reduced in proposed approach.

Figure 6 shows results of deformation after 80 s was elapsed. We can find that the results of corotated FEM were very similar to the result of NL-FEM. L-FEM remained larger in volume than the other approaches. Figure 7 and Figure 8 show results of errors of the displacement of a node whose initial position was (32, 32, 192). These errors were calculated by comparing with the NL-FEM. Maximum error of corotated FEM was under 3.6 mm. Even in the case of using the rotation of higher hierarchical level of tetrahedra, no significant error was observed. In contrast, an error of L-FEM was 22 mm.

Thus, the effectiveness of our proposed approach was confirmed.

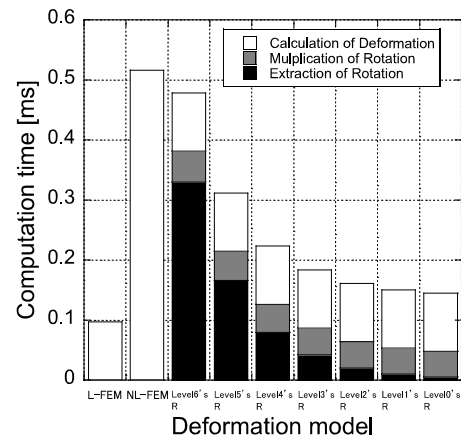


Figure 5. Computation Time.

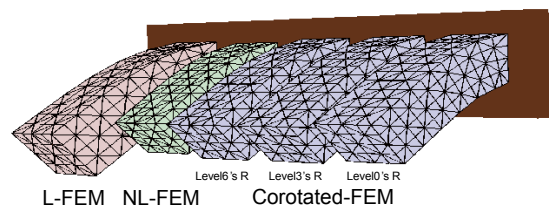


Figure 6. Deformation.

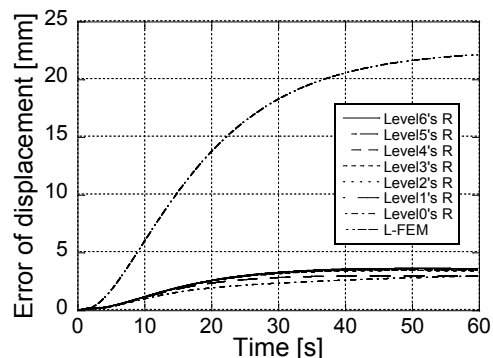


Figure 7. Error of Displacement.

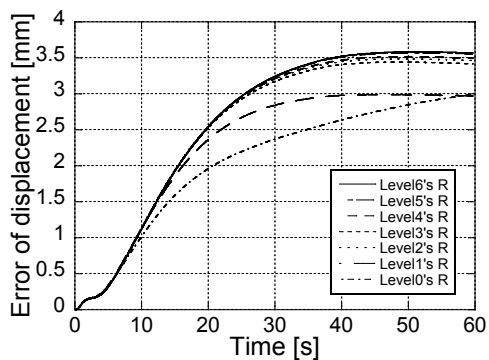


Figure 8. Error of Displacement (closeup).

V. DISCUSSION

A. Further Evaluation

In the previous section, simulation results of L-FEM and the proposed approach were compared to those of NL-FEM. In general, the errors of simulation results are caused by the accuracy of physical model, resolution of mesh and time step, shape and order of the elements. Also errors may occur depending on whether the material or geometrical nonlinearity is considered or not, and which numerical solution (e.g. Euler, Runge-Kutta, implicit) is used.

In the experiment, we confirmed that the accuracy of geometric nonlinearity only. In future, we are going to perform further evaluation experiments to confirm the accuracy of the physical model, and so on.

B. Consideration of Anisotropy

Also, in the previous section, we did not mention the result of the edge based StVK model [5-6]. In fact, the computation time of the edge based StVK model was about the same as the proposed model. However, the edge based StVK model has one drawback which is consideration of anisotropy is difficult. In contrast, our approach is able to consider the anisotropy.

C. Consideration of Arbitrary Object Shape

We are developing an adaptive and embedded deformation model in order to realize the real-time simulation of complex inhomogeneous objects such as organs which have arbitrary object shapes and inhomogeneous physical properties [20]. This approach would be able to use in the proposed approach.

D. Further Acceleration

In recent years, computational capability of many core processors, i.e. CPU, GPU or FPGA have reached new heights of numeric capacity. We are developing efficient computation procedures and data structure of this approach for GPU. In the future, further acceleration will be possible.

VI. CONCLUSION

In this paper, a novel efficient computation approach for the corotated FEM was proposed. We introduced several computation reduction techniques, as follows: 1) an efficient calculation approach for computing internal forces of nodes of elastic objects to take advantage of the rectangularity of the tetrahedral adaptive mesh; 2) fast shape matching approach by using a new scaling of polar decomposition; 3) an approach

for the reduction of the number of times of the shape matching by using the hierarchical structure.

In our evaluation experiment, we compared the accuracy of the deformation and the computation time among 1) proposed approach, 2) L-FE, and 3) NL-FEM, and then we showed the effectiveness of our proposed approach.

ACKNOWLEDGMENT

This work was partly supported by KAKENHI Grant Numbers 24500158, 24240020 and the SCOPE, Japan.

REFERENCES

- [1] A. Norton, G. Turk, B. Bacon, J. Gerth, and P. Sweeney. Animation of fracture by physical modeling. *Visual Computer*, Vol. 7, pp.210-219, 1991.
- [2] G. Yagawa and S. Yoshimura. *Computational dynamics and CAE Series 1: Finite Element Method*. Baifu-kan, Tokyo, 1991.
- [3] Y. Kobayashi, M. G. Fujie. *Organ Model Based Surgical Robot System*. J. Japanese Society for Medical and Biological Engineering, 49(5), pp.651-655, 2011.
- [4] Y.C.Fung. *Biomechanics: Mechanical properties of living tissues*. Springer, 1993.
- [5] H.Delingette. Biquadratic and quadratic springs for modeling St Venant Kirchhoff materials. *Proc. ISBMS*, pp.40-48, 2008.
- [6] R.Kikuuwe, H.Tabuchi and M.Yamamoto: An edge-based computationally efficient formulation of Saint Venant-Kirchhoff tetrahedral finite elements. *ACM Trans. Graph.*, Vol. 28, pp. 1-13, 2009.
- [7] M. Muller, J. Dorsey, L. McMillan, R. Jagnow, and B. Cutler. Stable real-time deformations. *Proc. ACM SCA*, pp.49-54, 2002.
- [8] A. McAdams, Y. Zhu, A. Selle, M. Empey, R. Tamstorf, J. Teran, and E. Sifakiss. Efficient elasticity for character skinning with contact and collisions. *Proc. ACM SIGGRAPH*, 30(4), pp.37:1-37:12, 2011.
- [9] C. Paloc, A. Faraci, F. Bello. Online remeshing for soft tissue simulation in surgical training. *IEEE Computer Graphics and Applications*, vol. 26, pp. 24-34, 2006.
- [10] G. DeBunne, M. Desbrun, M.-P. Cani, A. H. Barr. Dynamic real-time deformations using space & time adaptive sampling. *Proc. ACM SIGGRAPH*, pp.31-36, 2001.
- [11] H. T. Tanaka, Y. Tsujino, T. Kamada, H. Q. H. Viet. Bisection refinement-based real-time adaptive mesh model for deformation and cutting of soft objects. *Proc. ICARCV*, pp. 1-8, 2006.
- [12] S. Tomokuni, S. Hirai. Real-time simulation of rheological deformation on FPGA. *Journal of the Virtual Reality Society of Japan*, Vol. 10, No. 3, pp.443-452, 2005.
- [13] A. Rasmusson, J. Mosegaard, T. S. Sørensen. Exploring parallel algorithms for volumetric mass-spring-damper models in CUDA. *Proc. ISBMS*, pp.49-58, 2008.
- [14] O. Comas, Z. Taylor, J. Allard, S. Ourselin, S. Cotin, J. Passenger. Efficient nonlinear FEM for soft tissue modelling and its GPU implementation within the open source framework SOFA. *Proc. ISBMS*, pp.28-39, 2008.
- [15] E. Hermann, B. Raffin, F. Faure, T. Gautier, J. Allard. Multi-GPU and Multi-CPU Parallelization for Interactive Physics Simulations. *Proc. EuroPar*, pp.235-246, 2010.
- [16] H. Courtecuisse, H. Jung, J. Allard, C. Duriez. GPU-based real-time soft tissue deformation with cutting and haptic feedback, *Journal of Progress in Biophysics and Molecular Biology*, Vol.103, pp.159-168, 2010.
- [17] H. T. Tanaka, Y. Takama, H. Wakabayashi. Accuracy-based sampling and reconstruction with adaptive grid for parallel hierarchical tetrahedrization. *Proc. VG*, pp.79-86, 2003.
- [18] R. Byers and H. Xu. A new scaling for newton's iteration for the polar decomposition and its backward stability. *SIAM J. Matrix Anal. Appl.*, 30(2), pp.822-843, 2008.
- [19] G. M. Nielson and R. Franke. Computing the separating surface for segmented data, *Proc. of VIS'97*, pp.229-233, 1997.
- [20] K. Tagawa, T. Oishi, H. T. Tanaka. Adaptive and embedded Deformation Model: an approach to haptic interaction with complex inhomogeneous elastic objects, *Proc. IEEE WHC*, 2013.